Received: 5 May 2023 | Revised: 25 August 2023 | Accepted: 9 October 2023

DOI: 10.1002/pmic.202300212

Proteomics
Proteomics and Systems Biology

RESEARCH ARTICLE

Uncovering the proximal proteome of CTR1 through TurboID-mediated proximity labeling

Yuan-Chi Chien[1,2] | Andres Reyes[3,4] | Hye Lin Park[1,2] | Shou-Ling Xu[3,4] | Gyeong Mee Yoon[1,2]

[1]Department of Botany and Plant Pathology, Purdue University, West Lafayette, Indiana, USA

[2]The Center for Plant Biology, Purdue University, West Lafayette, Indiana, USA

[3]Department of Plant Biology, Carnegie Institution for Science, Stanford University, Stanford, California, USA

[4]Carnegie Mass Spectrometry Facility, Carnegie Institution for Science, Stanford, California, USA

Correspondence
Gyeong Mee Yoon, Department of Botany and Plant Pathology, Purdue University, West Lafayette, IN 47907, USA.
Email: yoong@purdue.edu

Funding information
National Science Foundation, Grant/Award Numbers: MCB1817286, IOS2245525, R01GM135706; National Institutes of Health, Grant/Award Number: R01GM135706

Abstract

Protein-protein interactions play a crucial role in driving cellular processes and enabling appropriate physiological responses in organisms. The plant hormone ethylene signaling pathway is complex and regulated by the spatiotemporal regulation of its signaling molecules. Constitutive Triple Response 1 (CTR1), a key negative regulator of the pathway, regulates the function of Ethylene-Insensitive 2 (EIN2), a positive regulator of ethylene signaling, at the endoplasmic reticulum (ER) through phosphorylation. Our recent study revealed that CTR1 can also translocate from the ER to the nucleus in response to ethylene and positively regulate ethylene responses by stabilizing EIN3. To gain further insights into the role of CTR1 in plants, we used TurboID-based proximity labeling and mass spectrometry to identify the proximal proteomes of CTR1 in *Nicotiana benthamiana*. The identified proximal proteins include known ethylene signaling components, as well as proteins involved in diverse cellular processes such as mitochondrial respiration, mRNA metabolism, and organelle biogenesis. Our study demonstrates the feasibility of proximity labeling using the *N. benthamiana* transient expression system and identifies the potential interactors of CTR1 in vivo, uncovering the potential roles of CTR1 in a wide range of cellular processes.

KEYWORDS
CTR1, ethylene, *N. benthamiana*, proximity labeling, TurboID

1 | INTRODUCTION

Ethylene is an essential growth regulator that influences various aspects of plant growth and development, as well as the plant's response to stress through interactions with other growth regulators and environmental factors [1]. The underlying mechanisms of ethylene signaling have been extensively studied, primarily through molecular genetics in *Arabidopsis* [2]. Recent studies have also demonstrated that the complicated regulation of the ethylene signaling pathway is achieved through the spatial and temporal regulation of the ethylene signaling components [3–8]. Ethylene is perceived by ethylene receptors on the endoplasmic reticulum (ER) membrane. When ethylene is present, ethylene inactivates the receptors and Constitutive Triple Response 1 (CTR1), an Raf-like protein kinase, reducing the phosphorylation of Ethylene Insensitive 2 (EIN2), a positive regulator of the ethylene response. This triggers the cleavage and transport of the C-terminal domain of EIN2 (EIN2-CEND) into the nucleus, where it activates the EIN3 transcription factor and its paralog EIN3-like 1 (EIL1) and regulates the transcriptional response to ethylene [8–11]. EIN2-CEND is also targeted to processing bodies (P-bodies), which are

cytoplasmic foci that regulate mRNA stability and translation, thereby regulating mRNA metabolism. EIN2-CEND binds to the untranslated region of *EBF* mRNA, inhibiting its translation and removing the suppression on the EIN3 transcription factor, enabling ethylene responses to occur [4, 6]. Our recent study has revealed that, similar to EIN2, CTR1 translocates from the ER to the nucleus upon sensing ethylene [5]. The nuclear movement of CTR1 occurs independently of EIN2, EIN3/EIL1, and its kinase activity. When CTR1 enters the nucleus, it binds to EIN3-Binding F-Box protein 1 (EBF1) and EBF2, leading to an increased level of EIN3 protein and, thus, positively regulating ethylene responses [5]. However, the mechanism by which CTR1 downregulates EBFs to enhance EIN3 protein abundance and how it enters the nucleus remain unknown.

CTR1 lacks transmembrane domains or targeting sequences for specific organelles; its ER localization results from the interaction with the cytosolic domain of the ethylene receptors, which are tethered to the ER through transmembrane domains [10]. The movement of CTR1 from the ER to the nucleus implies that CTR1 has the potential to be involved in various cellular processes by altering its subcellular localization or interacting with other proteins in response to various stimuli. To gain a better understanding of the roles of CTR1 and ethylene signaling in cellular processes, further research is needed, including the identification of its interacting proteins. This could provide additional insights into its interactions with other signaling pathways within the cell.

Approximately 80% of cellular proteins function as part of complexes or multi-protein assemblies [12]. Hence, identifying these interactions in vivo is crucial for comprehending the intricate dynamics of signaling pathways and how they respond to various environmental stimuli. Among the many techniques available to investigate protein-protein interactions, affinity purification-mass spectrometry (AP-MS) is widely used as an approach for identifying interacting proteins [13, 14]. AP-MS utilizes specific binding interactions, such as antibodies, to purify a complex mixture of proteins, which are then analyzed by mass spectrometry to identify the individual proteins present. This technique is frequently used to study both known and unknown interactions, making it a valuable tool for a wide range of applications in biochemistry and molecular biology [14, 15]. However, despite its advantages, AP-MS also presents several limitations. These limitations include limited sensitivity due to the potential removal of transient or weak interactors, as well as limited specificity resulting from the absence of spatial and temporal information regarding protein-protein interactions. Additionally, sample preparation processes can be challenging, requiring careful selection of appropriate affinity tags or antibodies, optimization of cell lysis, and pull-down procedures [16]. The recently developed proximity labeling technique offers a potential solution to some of the limitations of AP-MS [17–20]. Proximity labeling enables the identification of proteins that are in close proximity to the target protein of interest [21, 22]. This is achieved by using an engineered biotin ligase that is fused to the protein of interest. In the presence of biotin and ATP, the biotin ligase covalently attaches biotin to nearby proteins, which can then be affinity-purified using streptavidin-coupled beads and analyzed by mass spectrometry [18–20]. Proximity labeling offers several advantages that complement the drawbacks of the AP-MS approach. Firstly, it allows for identifying proteins in close proximity to a specific target protein or organelle at a particular time point or under specific conditions, providing spatial and temporal information about protein-protein interactions and localization that may not be captured using traditional AP-MS approaches. Secondly, proximity labeling captures protein-protein interactions based on physical proximity rather than relying on direct or indirect interaction affinity, enabling the identification of not only direct binding proteins but also proteins that are part of the same complex as the bait protein. Thirdly, proximity labeling can capture weak or transient interactions that are often lost during conventional affinity purification steps. This advantage allows for identifying more dynamic and regulatory protein interactions, which may be crucial for understanding cellular processes. Lastly, the proximity labeling approach is highly adaptable for various experimental setups, including in vivo labeling, organelle-specific labeling, and subcellular compartment analysis, allowing the study of protein interactions and localization in diverse biological contexts [18]. Proximity labeling has also been combined with other techniques, such as super-resolution microscopy, to study protein interactions at the single-molecule level, providing an even more detailed picture of protein-protein interactions in cells [23]. Overall, proximity labeling offers a powerful and complementary approach to AP-MS, providing additional insights into the spatial and temporal aspects of protein-protein interactions and localization within the cellular context.

In this study, we combined TurboID-based proximity labeling with a transient expression system to identify a group of proteins that form functional complexes with CTR1 in vivo [19, 22]. Our study has revealed that besides the ER, nucleus, and cytosol, which are previously known CTR1 localizations, CTR1 proximal proteins are also

Significance Statement

The spatiotemporal regulation of signaling molecules is essential for proper cellular responses and, ultimately, the survival of the organism. In the ethylene signaling pathway, CTR1 acts as a key regulator of the ethylene response, and its subcellular localization can be altered from the ER to the nucleus in response to ethylene. Our results reveal that CTR1 engages in proximal interactions with proteins localized in diverse subcellular compartments, suggesting contributions to specific cellular processes, such as carbon metabolism and post-transcriptional regulation. These findings imply that CTR1 has a multifaceted role in various cellular processes beyond the ethylene signaling pathway. Furthermore, our study demonstrates the successful implementation of TurboID-based proximity labeling, which is a highly active area of protein-protein interaction research in other systems but has only recently been introduced in plants.

found in various cellular compartments, such as mitochondria, P-body, cytoskeleton, peroxisome, and plasma membrane. These results imply that CTR1, in addition to regulating the ethylene signaling, might also have a significant impact on cellular processes such as energy metabolism, mRNA metabolism, organelle function, and cytoskeleton organization, which have not been previously reported.

2 | MATERIALS AND METHODS

2.1 | TurboID constructs

The infusion cloning strategy (Takara Bio, USA) was used to construct the plasmids used in this study (Table S1). The 1 kb *CTR1* promoter (*pCTR1*) and the CTR1 gene (*gCTR1*) were amplified from *Arabidopsis* genomic DNA. The GFP gene was amplified from the pSITE-2CA Gateway vector. The *pCTR1-GFP-gCTR1* and *pCTR1-GFP* constructs were created using the overlapping PCR method, and then cloned into StuI and XbaI sites in the pEarleyGate 104 vector. The ORF of *TurboID* was amplified from the *R4pGWB601_UBQ10p-TurboID-YFP-NLS* vector (addgene) and cloned into PacI and SpeI sites in the pEarleyGate 104 derived vectors via the Infusion method, resulting in *pCTR1-GFP-gCTR1-TurboID/pEarleyGate104* and *pCTR1-GFP-TurboID/pEarleyGate104*. All constructs were confirmed by Sanger sequencing.

2.2 | Subcellular localization of the TurboID-fused proteins

The leaves of *N. benthamiana* were infiltrated with *Agrobacterium* GV3101 carrying plasmids expressing TurboID-fused GFP-CTR1 or GFP. Three days later, the leaves were examined using a Zeiss 880 upright confocal microscope. To confirm nucleus and ER localizations, the nucleus marker bZip-BFP and the ER marker ER-RK were co-expressed with the TurboID-fused proteins.

2.3 | Optimization of biotin treatment conditions

Three days after infiltrating *N. benthamiana* leaves with *Agrobacterium* GV3101 carrying constructs for protein expression, the leaf tissue was harvested and cut into 1 cm x 1 cm squares for the biotin labeling. The tissue was submerged in sterilized water containing various biotin concentrations (0, 10, 50, 100 μM) for different periods of time (0, 15, 30, 60, 120 min) while being rotated on an end-over-end rotor wheel. After biotin treatment, the leaf tissue was blotted dry and snap-frozen for later analysis. The proteins from the leaf tissue were extracted by grinding them with the SDS-PAGE sample buffer and then subjected to immunoblotting with anti-streptavidin-HRP and anti-GFP antibodies, followed by staining with Coomassie blue.

2.4 | Sample preparation processing and LC-MS/MS

A total of four biological replicates for the two samples (GFP-CTR1-TurboID and GFP-TurboID) were prepared in two individual experiments, with two replicates in each. The protein expression in *N. benthamiana* and biotin treatment were done with the leaf fragments being treated with 50 μM biotin for 120 min. After biotin treatment, 1 g of finely ground *N. benthamiana* leaf tissue was resuspended in 2 mL of ice-cold extraction buffer (50 mM Tris pH 7.5, 150 mM NaCl, 0.1% SDS, 1% Triton-X-100, 0.5% Na-deoxycholate, 1 mM EGTA, 1 mM DTT, 1x complete protease inhibitor, and 1 mM PMSF), sonicated in an ice bath for 2 min (10 sec on/ 10 sec off). All subsequent steps were done on ice or at 4°C. The tissue suspensions were centrifuged at 1,500 rpm for 5 min to remove debris. The supernatant was then centrifuged again at 12,000 rpm for 10 min to remove further debris. The extracts were first desalted using a PD-10 desalting column to remove free biotin (Cytiva). Next, the protein extract was incubated overnight with a 200 μL bead slurry of MyOne Streptavidin C1 (Invitrogen), which was pre-washed with an extraction buffer on a rotor wheel. The beads were washed with cold extraction buffer (50 mM Tris pH 7.5, 150 mM NaCl, 0.1% SDS, 1% Triton-X-100, 0.5% Na-deoxycholate, 1 mM EGTA, and 1 mM DTT), 1 M KCl, 100 mM Na_2CO_3, and 2 M urea in 10 mM Tris (pH 8) at room temperature and shipped to the MS facility on ice.

For on-beads tryptic digestion, the streptavidin beads were washed with 1x cold 1 M KCl, 1 × 2 M Urea in 10 mM Tris-HCL pH 8, and 2x cold 50 mM Tris pH 7.5, 2x with Urea wash buffer 3 (50 mM Tris pH 7.5, 1 M Urea), followed by three hours of incubation in Trypsin buffer (50 mM Tris pH 7.5, 1 M Urea, 1 mM DTT, 0.4 μg Trypsin) at 25°C. The supernatant from tryptic digestion and two washes with 60 μL 1 M Urea in 50 mM Tris pH 7.5 were reduced, alkylated, and digested overnight with 0.5 μg Trypsin. Another 0.5 μg of trypsin was added the next morning, followed by acidification four hours later by adding formic acid to a final concentration of ∼1% and desalting using OMIX C18 pipette tips (A57003100).

LC-MS/MS was done on a Q-Exactive HF hybrid quadrupole-Orbitrap mass spectrometer (Thermo Fisher), equipped with an Easy LC 1200 UPLC liquid chromatography system (Thermo Fisher). Peptides were first trapped using a trapping column (Acclaim PepMap 100 C18 HPLC, 75 μm particle size, 2 cm bed length), then separated using an analytical column (Acclaim PepMap 100 C18 HPLC (2 μm particle size, 25 cm bed length) (Thermo Fisher). The flow rate was 300 nL/min and a 120-min gradient was used. Peptides were eluted by a gradient from 3 to 28% solvent B (80% acetonitrile, 0.1% formic acid) over 100 min and from 28% to 44% solvent B over 20 min, followed by a short wash at 90% solvent B. The precursor scan was from a mass-to-charge ratio (m/z) of 375 to 1,600 and the top 20 most intensely charged precursors were selected for fragmentation. Peptides were fragmented with higher-energy collision dissociation (HCD) with normalized collision energy (NCE).

2.5 | MS data processing and statistical analysis

Mass spectrometry data was searched using MaxQuant for Label-Free Quantification (LFQ) and Protein Prospector for peptide counting. A MaxQuant (ver. 1.6.2.10) search was executed using default parameters with the following changes: In group-specific parameters, LFQ was enabled with "Fast LFQ" checked. In global parameters, "Match between runs" was enabled. For Identification, peptides were searched against the Uniprot-proteome_UP000084051 protein database (downloaded 10/06/21) obtained from Uniprot containing a total of 73,606 entries. The proteingroups.txt file output from MaxQuant was analyzed in Perseus (ver. 1.6.15.0). LFQ intensities were imported and filtered with the following features: removing 'reverse = +', 'potential contaminant = +', and 'only identified by site = +'. Data was log2 transformed and rows that were not identified in at least three replicates of one sample group were removed. Missing values were imputed from a normal distribution (width = 0.3, downshift = 1.8, total matrix mode). A student's t-test was executed to examine the statistics between GFP-CTR1-TurboID and GFP-TurboID control. The t-test settings were the following: 'Permutation-based FDR', 'FDR = 0.1′, S0 = 2, 'Report q-value', 'Number of Randomizations = 250′, and '−log10 *p*-value'. Data was searched using Protein Prospector (ver. v 6.2.1). The data was searched against the same database, UniProtKB.UP000084051_4097 protein database concatenated with randomized peptides to calculate FDR. Spectral counts were used to analyze the data.

The statistical cut-offs ($-\log_{10}$ (*P*-value) > 2 and $\log_2$ (fold change) > 1) were used to identify the proteins that were significantly more abundant in GFP-CTR1-TurboID compared to GFP-TurboID control. The proteins that are statistically more abundant in GFP-CTR1-TurboID were selected as CTR1 proximal proteins. Additionally, a principal component analysis (PCA) was performed using Perseus. The Venn diagrams, which show the overlapping proteins found in the four replicates of the two samples, were made using InteractiVenn [24].

2.6 | Classification of the subcellular localizations and functions of the proximal proteins

After identifying CTR1 proximal proteins in *N. benthamiana*, we retrieved their complete protein sequences from the Uniprot database [25] using the accession numbers obtained from MaxQuant. We used the NCBI Protein BLAST to search for the Arabidopsis homologs of these proteins. The subcellular localization was determined through manual searches in the Uniprot database and the literature.

To analyze the functional clustering of the CTR1 proximal proteins, we imported the *Arabidopsis* gene IDs of the 27 protein candidates identified in this study, as well as, CTR1 to STRING version 11.5 [26], with the minimum required interaction score set to "medium confidence (0.400)". The STRING network image was then exported from the STRING website.

The proteins involved in pyruvate decarboxylation and the TCA cycle were searched on the Plant Metabolic Network (PMN) [27]. The figure depicting the super pathway of cytosolic glycolysis (plants), pyruvate dehydrogenase, and the TCA cycle was exported from the PMN website, and the five CTR1 proximal proteins involved in the pathway were manually annotated on the figure.

2.7 | BiFC and co-immunoprecipitation

For the bimolecular fluorescence complementation (BiFC) assay, leaves of *N. benthamiana* were infiltrated with *Agrobacteria* GV3101 carrying plasmids expressing BFP-bZIP (a nucleus marker and an expression control), nYFP-CTR1, and the indicated cYFP-fused protein. CIP8 was used as a negative control. Three days after infiltration, the leaves were examined using a Zeiss 880 upright confocal microscope. For the co-immunoprecipitation (co-IP) assay, *Arabidopsis* protoplasts were isolated and transfected with indicated plasmids using the PEG method [28]. Sixteen hours post-transfection, protoplasts were harvested and lysed in RIPA buffer (10 mM Tris-HCl, pH 8.0, 1 mM EDTA, 0.5 mM EGTA, 1% Triton X-100, 0.1% Sodium Deoxycholate, 0.1% SDS, 140 mM NaCl) supplemented with protease inhibitor cocktail and 1 mM PMSF for 30 min. The input sample was collected, and the remaining protoplast lysates were incubated with Pierce™ Anti-HA Magnetic Beads or ChromoTek GFP-Trap Magnetic Agarose for 2 hours at 4°C. Subsequently, the samples were washed with ice-cold PBS buffer three times before being eluted with 2x SDS sample buffer and subjected to immunoblotting.

3 | RESULTS

3.1 | CTR1-TurboID fusion protein localizes in the ER and nucleus in *N. benthamiana*

To identify the protein interactome of CTR1 in vivo and uncover potential interacting partners, we utilized TurboID, an improved variant of the bacterial biotin ligase biotin retention A (BirA). TurboID has been successfully utilized in various biological systems, including yeast, plants, and animals [20, 22]. To test the biotin ligase activity of TurboID and perform proximity labeling of CTR1 in *N. benthamiana* leaves, we constructed a binary vector containing a 7.6 Kb genomic *CTR1* transgene consisting of a *CTR1* promoter region driving expression of the CTR1 coding region fused to a GFP reporter at the N-terminus and TurboID at the C-terminus (*CTR1p:GFP-gCTR1-TurboID*) (Figure 1A). As a direct interacting partner of the ethylene receptors localized in the ER, CTR1 has been known to be predominantly localized to the cytosolic side of the ER. However, our recent study has revealed that CTR1 translocates into the nucleus in response to ethylene, indicating its localization in the cytoplasm and nucleus [5]. To remove non-specific-binding proteins that are co-localized with CTR1 in the cytoplasm and nucleus, we constructed a control binary vector containing a CTR1 promoter driving the expression of GFP-fused TurboID (GFP-TurboID), which served as cytosolic and nucleus controls due to the dynamic localization of CTR1. The *CTR1p:GFP-gCTR1-TurboID* transgene

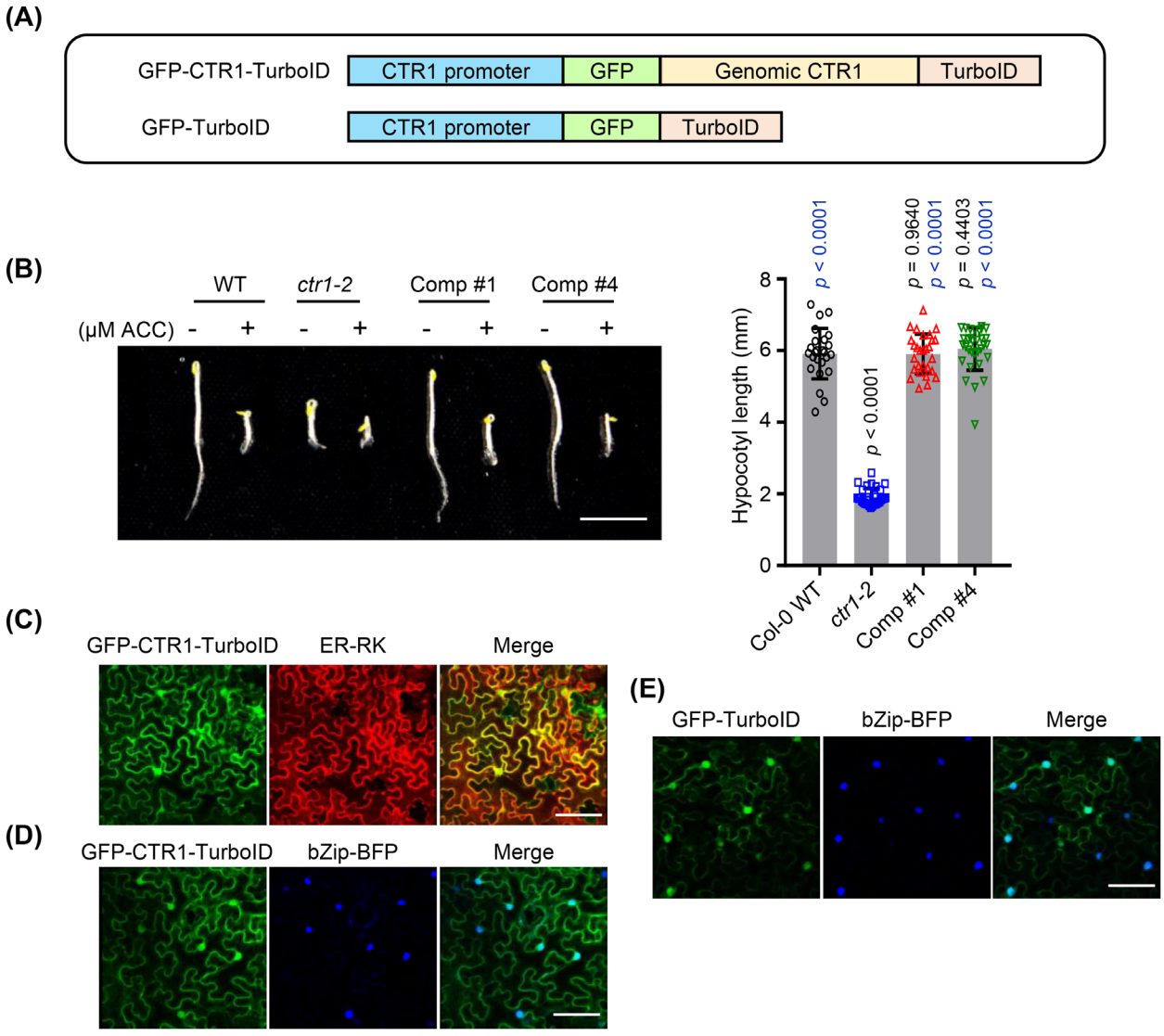

FIGURE 1 Complementation and subcellular localization of the TurboID-fused CTR1 protein. (A) A scheme of constructs used in this study. (B) Complementation of a *ctr1-2* null mutant by a *CTR1p:GFP-gCTR1-TurboID* transgene. *Arabidopsis* seedlings were grown in media supplemented with or without 10 μM ACC for 3 days in the dark. Scale bar, 5 mm. The graph represents the quantification of hypocotyl lengths of seedlings grown on MS without ACC. MS, Murashige and Skoog medium. Significance was determined by one-way ANOVA with Dunnett's multiple comparisons test to compare the results of the complementation lines to the WT (black) and *ctr1-2* (blue) controls. Error bars, SE ($n \geq 25$). (C-E) Subcellular localizations of GFP-TurboID-CTR1 and GFP-TurboID in *N. benthamiana* leaves. Tobacco leaves coexpressing GFP-CTR1-TurboID or GFP-TurboID proteins were imaged by a confocal microscope. bZip-BFP (a nuclear marker); ER-RK (an ER marker). Scale bars, 100 μm.

fully complemented *ctr1-2* (a null allele) in dark-grown *Arabidopsis* seedlings, indicating the fusion protein of CTR1 is functional in vivo (Figure 1B).

To confirm the subcellular localization of the engineered CTR1-TurboID fusion proteins, we transiently expressed these fusion proteins in *N. benthamiana* and observed their subcellular localizations. CTR1-TurboID was found to be localized in both the ER and nucleus (Figure 1C,D), while the control protein GFP-TurboID was localized to the nucleus and cytosol (Figure 1E). These results confirm that the addition of TurboID does not alter the subcellular localization of the CTR1 fusion protein, ensuring its use in identifying the in vivo protein interactomes of CTR1 in *N. benthamiana*. Additionally, the results indicate that GFP-TurboID is a suitable control for eliminating non-specific proximal proteins of CTR1.

3.2 | Optimization of proximity biotin labeling conditions in *N. benthamiana*

Optimizing the experimental conditions for biotin labeling is crucial for identifying potential interactors and the proximal proteome of a protein of interest. To evaluate biotin ligase activity and find optimal biotin labeling conditions, including labeling time and biotin concentrations, we infiltrated *N. benthamiana* leaves with *Agrobacteria* carrying

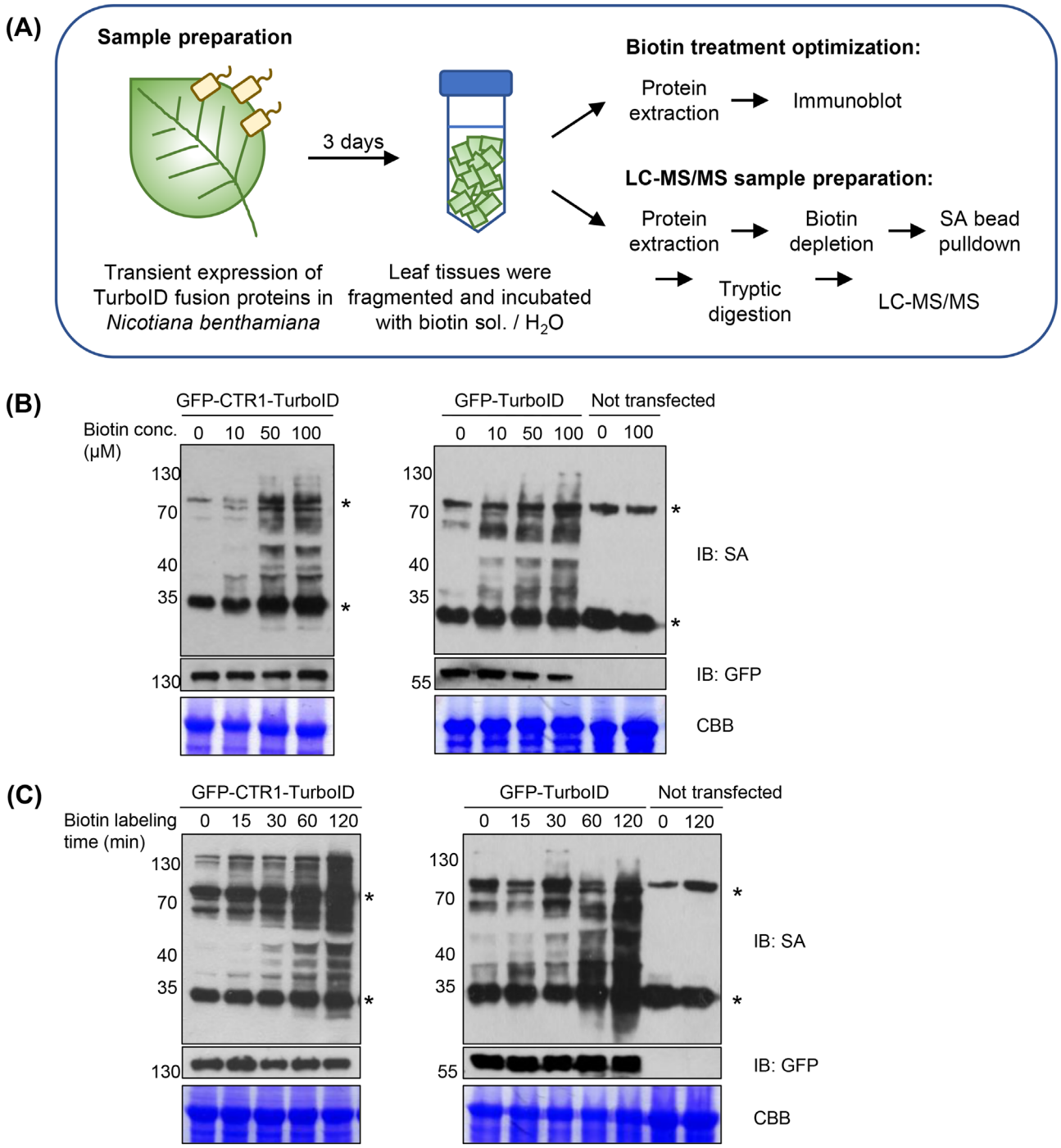

FIGURE 2 Optimization of TurboID-based biotinylation in *N. benthamiana*. (A) A workflow for biotin labeling and sample preparation for LC-LC/MS. (B) The correlation between the TurboID labeling efficiency and biotin concentrations. Fragmented transfected leaves were incubated with the indicated concentrations of biotin for 60 min, followed by immunoblot (IB) analysis using anti-streptavidin (SA) and anti-GFP antibodies. (C) Time-dependent activity of TurboID. Fragmented transfected leaves were incubated with 50 μM biotin for different durations, followed by immunoblot analysis to detect biotinylated proteins. Coomassie Brilliant Blue (CBB)-stained gel was used as the loading control. Not transfected tissues with and without biotin treatment are included as negative controls. Asterisks indicate naturally biotinylated proteins.

plasmids expressing GFP-CTR1-TurboID or GFP-TurboID. To determine the optimal concentration of biotin for TurboID, the infiltrated leaf tissues were incubated with biotin concentrations ranging from 1 to 100 μM for 1 h (Figure 2A,B). Analysis of total protein extracts containing GFP-CTR1-TurboID using immunoblotting showed only weak background labeling at 10 μM biotin, followed by a steep increase at 50 μM, and saturation at 100 μM (Figure 2B). Total protein extracts expressing GFP-TurboID showed similar biotin labeling patterns as GFP-CTR1-TurboID at different biotin concentrations (Figure 2B). These results suggest that a concentration of 50 μM

biotin is appropriate for optimal biotin labeling in *N. benthamiana*. We further determined the appropriate labeling time when using 50 μM biotin. Both of the two TurboID fusion proteins (CTR1-TurboID and GFP-TurboID) induced labeling of cellular proteins above background levels similarly within 30 min of treatment with 50 μM biotin at room temperature (22°C), with a sharp increase in labeling over the next 60 to 120 min (Figure 2C). Together, these results indicate that the optimal biotin labeling conditions for TurboID fusion proteins in *N. benthamiana* include a biotin concentration of 50 μM and 120 minutes of incubation at room temperature in our experimental setting.

3.3 | Identification of the proximal biotinylated proteins of CTR1

Through empirical testing of the critical steps of biotin labeling, we identified the optimal biotin concentration and incubation time in *N. benthamiana* (Figure 2). To proceed with the identification of proximal proteins of CTR1, we infiltrated *N. benthamiana* leaves with *Agrobacteria* carrying plasmids that express GFP-CTR1-TurboID or GFP-TurboID, followed by incubation in a growth chamber for 3 days. Afterward, the infiltrated leaves were treated with 50 μM biotin for 120 min and washed with ice-cold water to stop labeling and remove excess biotin. The total protein extracts were then passed through PD-10 gel filtration to remove unbound biotin. After purifying the biotinylated proteins using magnetic streptavidin beads, we analyzed them using liquid chromatography-tandem mass spectrometry (LC-MS/MS) to identify and quantify the captured proteins (Figure 2A). We prepared four biological replicates of *N. benthamiana* leaves expressing different TurboID fusion proteins in two independent experiments, with two replicates in each experiment. Principal component analysis (PCA) showed a clear separation of the GFP-CTR1-TurboID samples from the GFP-TurboID control, and Venn diagrams of the four biological replicates for each sample showed significant overlap of proteins, indicating the reproducibility of the experimental method (Figure S1A,B). To identify the list of CTR1 proximal proteins enriched in GFP-TurboID-CTR1 samples, we selected proteins that were present in at least three replicates in each sample for statical analysis and used statistical cut-offs of P-value < 0.01 and fold change > 2 for identifying proteins enriched in GFP-TurboID-CTR1 samples (Figure 3A, Table 1, and Table S2). The proteins that were not enriched in GFP-TurboID-CTR1 or found in both GFP-TruboID-CTR1 and GFP-TurboID samples with similar abundance likely consist of non-specifically binding proteins and proteins that are natively biotinylated by biotin ligases expressed in *N. benthamiana*. After applying this filtering step, we identified 27 proteins that were significantly more abundant in GFP-CTR1-TurboID. (Figure 3B). Subsequently, we searched the Uniprot database for protein sequences of the identified 27 protein candidates using accession numbers from MaxQuant and imported the results into NCBI Protein BLAST to find *Arabidopsis* homologs (Table 1 and Table S2).

3.4 | Analysis of the identified proximal proteins of CTR1

Further analysis was carried out on the 27 "high-confidence" candidate proteins to examine their protein-protein association networks using STRING version 11.5 [26], with the minimum required interaction score set to "medium confidence (0.400)". This analysis revealed that the CTR1 proximal proteins were divided into various subcellular localizations and functional categories, including but not limited to the ethylene signaling pathway, mitochondrial respiration, protein chaperone, mitochondria, and peroxisome biogenesis, carbon catabolite repression 4 (Ccr4)-negative TATA-less (NOT) (CCR4-NOT) complex, and microtubule binding (Figure 3C). Of the 27 candidates, Ethylene Receptor 1 (ETR1), which is a known CTR1-interacting protein, was enriched, supporting the validity of the workflow. Another known CTR1 interactor, Ethylene Insensitive 2 (EIN2) was also identified in the analysis. However, possibly due to the highly dynamic characteristic of the protein, EIN2 was not only highly biotinylated in the GFP-CTR1-TurboID sample but also in the control GFP-TurboID, resulting in lower statistical significance ($-\log_{10}$ (P-value) = 1.59 and $\log_2$ (fold change) = 0.69). CTR1 itself was significantly enriched in both filtering steps, indicating the self-biotinylation of GFP-CTR1-TurboID ($-\log_{10}$ (P-value) = 3.04 and $\log_2$ (fold change) = 6.67).

Notably, there are six candidate proteins that play a role in regulating respiration in mitochondria (Figure 3C, Table 1, Table S2, and Figure S2) [29, 30]. The identified proteins, including Dihydrolipoyl Dehydrogenase (LPD1), Pyruvate dehydrogenase (PDH1), Succinate Dehydrogenase Iron-Sulfur Subunit (SDH2-2), Succinate dehydrogenase subunit 5 (SDH5), Malic Enzyme (NAD-ME1) and Probable ATP synthase 24 kDa subunit, mitochondrial (MGP1) [29, 30], are crucial for maintaining the Tricarboxylic Acid (TCA) cycle flux. PDH1 and LPD1 are the E1 and E3 subunits of the Pyruvate Dehydrogenase Complex (PDC), respectively, which are essential for connecting glycolysis to the TCA cycle through converting pyruvate to acetyl-CoA. Dihydrolipoyl transferase, which is the E2 subunit of the PDC, was also identified in our samples although statistical significance was relatively low (Table S3). SDH and NAD-ME play important roles in maintaining the flux of the TCA cycle through the conversion of succinate to fumarate via oxidation reactions and control of the flux from malate to oxaloacetate, respectively. MGP1 is a subunit of the mitochondrial membrane ATP synthase, which is essential for ATP synthesis driven by the electron transport chain after the TCA cycle. The identification of two SDH proteins, NAD-ME and MGP1 further support that CTR1 might play a role in respiration. Interestingly, a mitochondrial inner membrane translocase subunit, TIM44-2, which is an essential component in the ATP-dependent mitochondrial protein import, was also identified as a candidate protein (Table 1).

In addition to the identification of mitochondrial proteins, Dynamin-Related Proteins 3A (DRP3A) and Dynamin-Related Proteins 3B (DRP3B) are two candidate proteins predicted to be localized in both mitochondria and peroxisomes. DRP proteins are critical components of the organelle division machinery shared by peroxisomal and

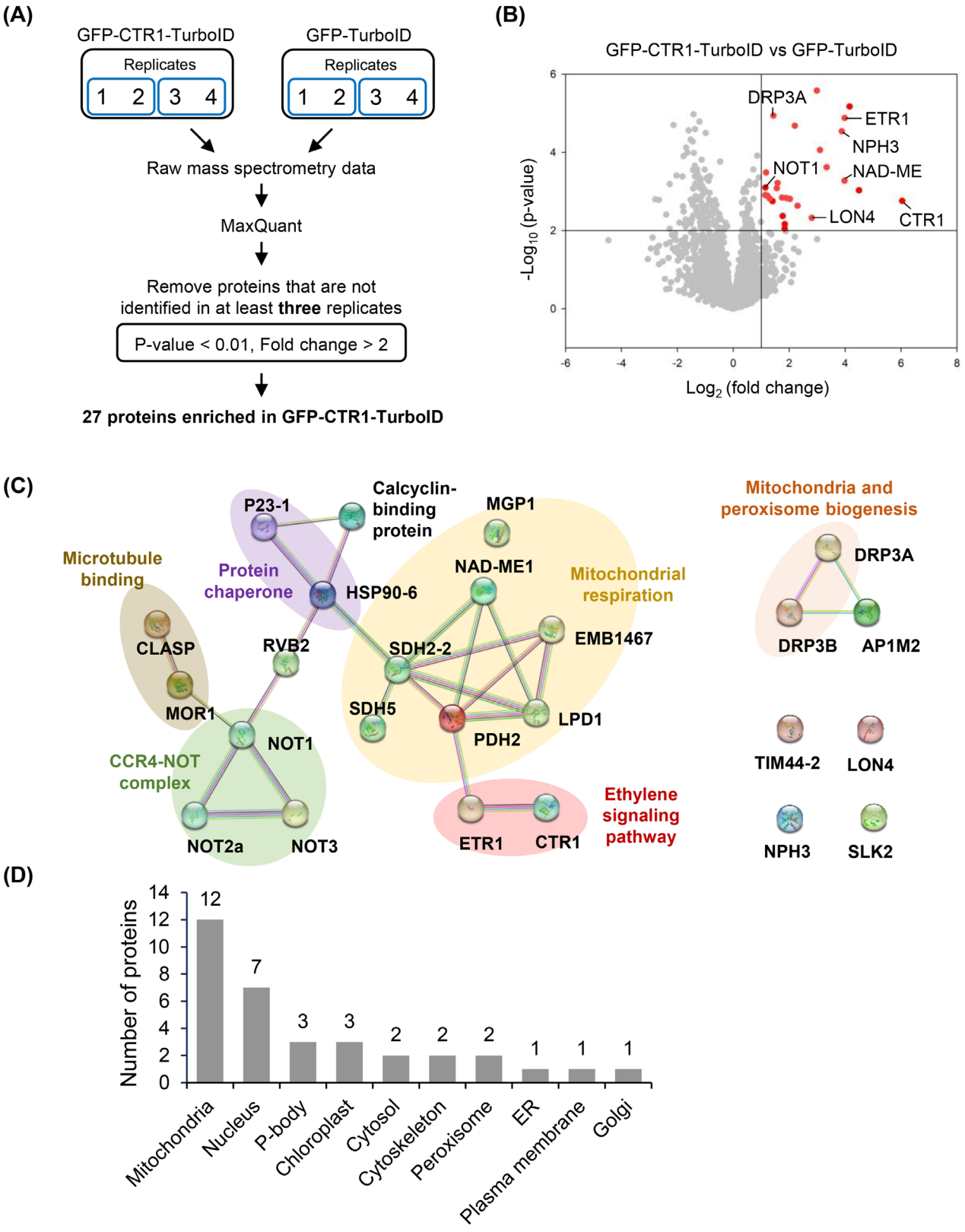

FIGURE 3 TurboID-mediated labeling reveals CTR1 proximal proteins. (A) Workflow of data analysis, filtering steps, and the numbers of proteins enriched in GFP-TurboID-CTR1 samples compared to GFP-TurboID samples. *P*-value < 0.01 and fold change > 2 were used as statistical standards to identify significantly enriched proteins. (B) Volcano plot of GFP-CTR1-Turbo versus GFP-Turbo. CTR1, ETR1, and proteins that were selected for BiFC analysis were labeled. Red dots indicated proteins enriched under the statistical standard of *P*-value < 0.01 and fold change > 2. (C) STRING analysis and functional clustering of the CTR1 proximal proteins. (D) Known or predicted subcellular localizations of the 27 proximal proteins. Proteins with more than one subcellular localization were counted repeatedly.

TABLE 1 List of identified CTR1 proximal proteins in this study.

	Gene name	Gene ID	Arabidopsis ortholog short name	Arabidopsis ortholog AGI	Subcellular localization
1	Ethylene receptor 1-like	LOC107824400	ETR1	AT1G66340	ER
2	Malic enzyme	LOC107775826	NAD-ME1	AT2G13560	MT
3	Root phototropism protein 3-like isoform X1	LOC107774889	NPH3	AT5G64330	PM
4	Succinate dehydrogenase subunit 5, mitochondrial-like	LOC107773166	SDH5	AT1G47420	MT
5	Mitochondrial import inner membrane translocase subunit TIM44-2-like	LOC107766603	TIM44	AT2G36070	MT
6	Co-chaperone protein p23	LOC107793601	P23-1	AT4G02450	N, CY
7	Lon protease homolog, mitochondrial	LOC107796400	LON4	AT3G05790	MT, CP
8	Calcyclin-binding protein	LOC107787168	T1P2	AT1G30070	N, CY
9	Probable NOT transcription complex subunit VIP2 isoform X2	LOC107771307	NOT2a	AT1G07705	N, PB
10	General negative regulator of transcription subunit 3 isoform X3	LOC107822036	NOT3	AT5G18230	N, PB
11	Protein MOR1-like	LOC107812666	MOR1	AT2G35630	CK
12	Pyruvate dehydrogenase E1 component subunit beta	LOC107815578	PDH2	AT5G50850	MT
13	Probable transcriptional regulator SLK2	LOC107797288	SLK2	AT5G62090	N
14	NADH dehydrogenase [ubiquinone] iron-sulfur protein 1, mitochondrial	LOC107808648	EMB1467	AT5G37510	MT, CP
15	Probable ATP synthase 24 kDa subunit, mitochondrial	LOC107807235	MGP1	AT2G21870	MT
16	Heat shock protein 90-6, mitochondrial-like	LOC107769814	HSP90-6	AT3G07770	MT
17	CLIP-associated protein-like	LOC107784908	CLASP	AT2G20190	CK
18	Dynamin-related protein 3A-like	LOC107793317	DRP3A	AT4G33650	MT, P
19	RuvB-like helicase	LOC107800852	RVB2	AT5G67630	N, CP
20	Succinate dehydrogenase [ubiquinone] iron-sulfur subunit, mitochondrial	LOC107802674	SDH2-2	AT5G40650	MT
21	Dynamin-related protein 3B-like isoform X2	LOC107828206	DRP3B	AT2G14120	MT, P
22	AP-1 complex subunit mu-2	LOC107816812	AP1M2	AT1G60780	ED, GG, CCV
23	CCR4-NOT transcription complex subunit 1-like isoform X2	LOC107804987	NOT1	AT1G02080	N, PB
24	Dihydrolipoyl dehydrogenase	LOC107821052	LPD1	AT1G48030	MT
25	Uncharacterized protein LOC107821945				
26	Uncharacterized protein OsI_027940-like				
27	Uncharacterized protein Os08g0359500-like isoform X2				

Abbreviations: CCV, Clathrin-coated vesicles; CP, chloroplast; CK, cytoskeleton; CY, cytosol; ED, endosome; ER, endoplasmic reticulum; GG, Golgi; MT, mitochondria; N, nucleus; P, peroxisome; PB, P-body; PM, plasma membrane.

mitochondrial divisions (Figure 3C and Table 1). Additionally, Lon protease 4 (LON4) was identified. Lon proteases belong to the evolutionarily conserved ATP-dependent protease family and are critical for plant organelle biogenesis and energy metabolism [31]. In *Arabidopsis*, LON isoforms are targeted to mitochondria, chloroplasts, and peroxisomes (Figure 3C and Table 1) [32]. Moreover, Non-Phototropic Hypocotyl 3 (NPH3) is also an identified candidate protein. NPH3 is known to localize at the plasma membrane and is involved in blue light signaling (Figure 3C).

One of the notable groups of candidates belongs to the CCR4-NOT complex (Figure 3C and Table 1) [33–35]. This complex is a large multiprotein structure that plays a vital role in post-transcriptional gene regulation in eukaryotic cells, both in the nucleus and within processing bodies (P-bodies) [35]. It comprises several subunits, including CCR4, CAF1, NOT1, NOT2, NOT3, and NOT4. We identified NOT1, NOT2a, and NOT3 as "high-confidence" protein candidates. As a core component of P-bodies, the Ccr4-NOT complex plays a key role in mRNA deadenylation by removing the poly(A) tail, causing destabilization and degradation [33, 35, 36]. Recent studies have shed light on the role of P-bodies in regulating ethylene responses [4, 6]. The identification of the CCR4-NOT complex components as proximal proteins of CTR1 highlights the significance of post-transcriptional regulation in ethylene responses and suggests a possible role for CTR1 in the process. Among the high-confidence candidates, seven proximal interactors, including the three CCR4-NOT complex proteins, a chaperone protein P23-1, a calcyclin-binding protein, the transcriptional regulator SLK2, and a RuvB-like helicase, are known or predicted to be localized in the nucleus, which aligns with CTR1's localization to the nucleus upon activation of the ethylene signaling pathway (Figure 3C, 3D, and Table 1) [5].

3.5 | Validation of direct interaction between CTR1 and its proximal proteins

The identified CTR1 proximal proteins from TurboID-mediated proximity labeling can form complexes with CTR1 through direct or indirect interaction [37]. To identify the direct interactors of CTR1 from the 27 high-confidence proteins, we selected five proteins, namely NAD-ME, DRP3A, LON4, NPH3, and NOT1, and tested their direct interaction with CTR1 using the Bimolecular Complementation (BiFC) assay. The reconstituted YFP fluorescence in *N. benthamiana* leaves showed that among the five tested CTR1 proximal proteins, NPH3 and DRP3A exhibited strong interactions with CTR1 (Figure 4A). NPH3 predominantly localizes to the plasma membrane under darkness but rapidly internalizes into aggregates upon blue light perception [38, 39]. This shift in localization is dependent on the phosphorylation status of NPH3 by the phototropin (phot) light-activated kinase (phot1) [40]. Consistent with the prior report, we observed that the reconstituted YFP signal resulting from the interaction between CTR1 and NPH3 was colocalized with the plasma membrane marker, PM-RK (Figure 4A and Figure S3A) [41]. Interestingly, we also observed cytosolic aggregation of the reconstituted YFP signal from CTR1 and NPH3 interactions in some cells, akin to observations in previous studies (Figure S3B) [38, 39]. This result suggests that CTR1 may be involved in regulating the phosphorylation status of NPH3. DRP3A, which is a key factor in mitochondrial and peroxisomal division and morphology, showed reconstituted YFP signals with CTR1 at cytosolic puncta in *N. benthamiana* (Figure 4A). Further co-localization analysis using the peroxisome marker, Px-RB [41], revealed that the interaction takes place at peroxisomes, consistent with the association of DRP3A with the cytosolic side of peroxisomes [42] (Figure S3C). The mitochondrial protein NAD-ME and the CCR4-NOT complex protein NOT1 were found to directly interact with CTR1, but their interaction intensity appeared to be weaker than that of the other candidates, yet still above that of the negative control CIP8. In contrast to the other CTR1 proximity proteins tested, LON4, which is known to be dually localized to mitochondria and chloroplasts, did not show any reconstituted YFP signals, suggesting no or indirect interaction with CTR1. We further selected the two proteins, NPH3 and DRP3A, which show strong reconstituted YFP signals in BiFC assays with CTR1, for the co-immunoprecipitation assay. The result showed that CTR1 is co-immunoprecipitated with both NPH3 and DRP3A, suggesting that CTR1 indeed interacts with these two proteins in vivo (Figure 4B,C).

4 | DISCUSSION

To understand the function of a protein, it is essential to investigate its subcellular localization and identify its interacting proteins. CTR1 has previously been reported to be localized in the cytosolic side of the ER membrane [43]. However, CTR1 lacks any predicted transmembrane domains and is known to dissociate from the ER in ethylene receptor loss-of-function mutants [10, 43]. This implies that the ER localization of CTR1 is likely due to its recruitment from the cytosol to ethylene receptors. Our recent study showed that CTR1 can move from the ER to the nucleus in response to ethylene, indicating its potential to change localization in response to different signals [5]. The proximal proteins of CTR1 identified in the study have diverse subcellular locations, including the ER, cytosol, nucleus, mitochondria, chloroplasts, Golgi, peroxisomes, processing body, and plasma membrane, agreeing with the release of CTR1 from the ER. The labeling radius of BioID, the original variant of TurboID, is estimated to be 10 nm, which is roughly the size of an average globular protein, but significantly smaller than the size of an organelle [18]. This implies that CTR1 is likely associated with the cytoplasmic compartments and organelles where the proximal proteins are localized. Taken together, these findings suggest that CTR1 may play roles in multiple cellular processes occurring in various subcellular compartments, providing new insight into the functions of CTR1 in plants.

Our analysis of the functional clusters of the CTR1 proximal proteins has revealed that a significant proportion of the identified proteins are mitochondrial proteins, especially proteins involved in mitochondrial respiration. The connection between the ethylene signaling pathway and mitochondria remains unclear. However, recent studies have demonstrated that ethylene exposure can lead to an

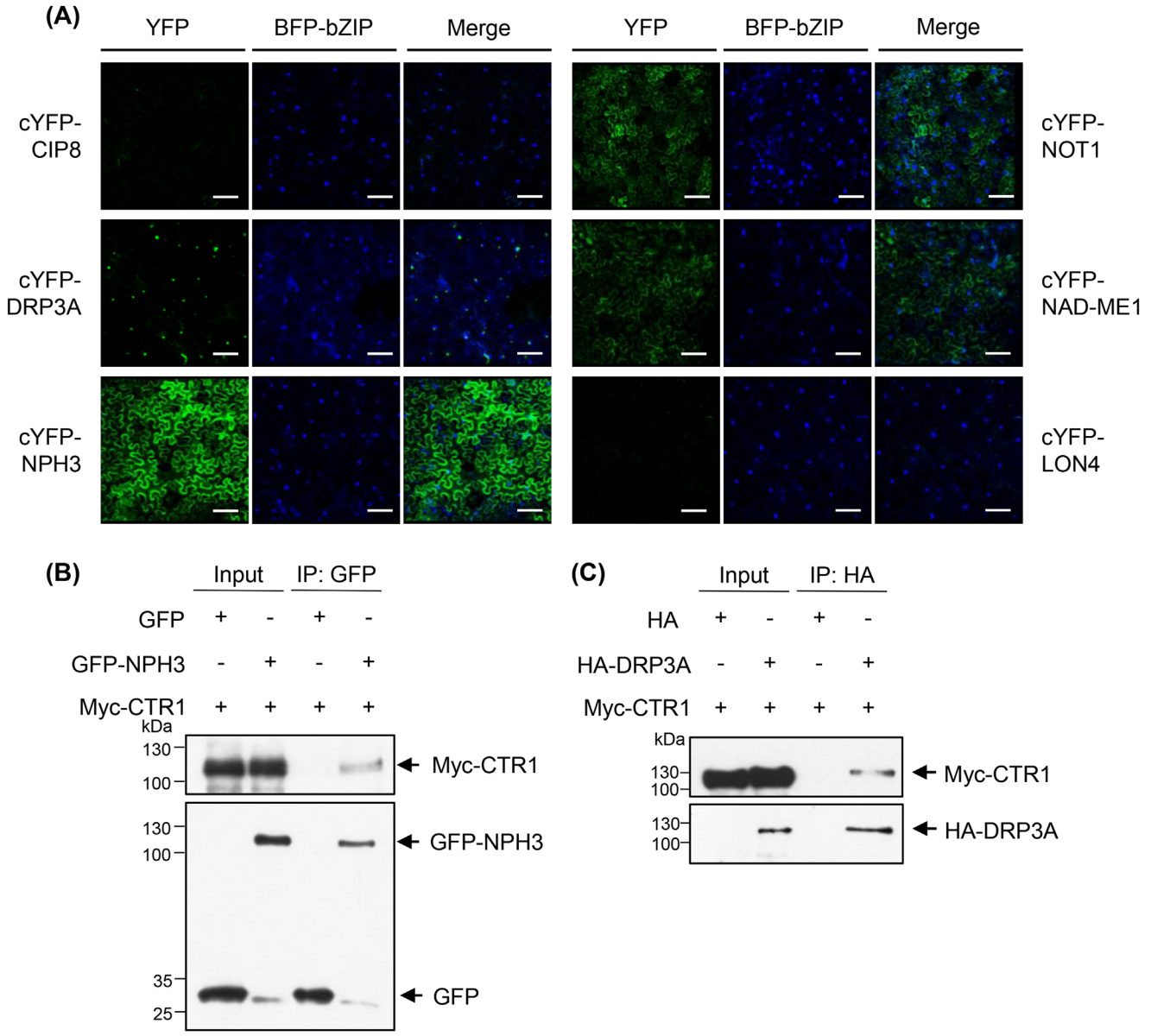

FIGURE 4 Validation of the direct interaction between CTR1 and the identified CTR1 proximal proteins in *N. benthamiana*. (A) BiFC of CTR1 and selected CTR1 proximal proteins. Leaves of *N. benthamiana* were infiltrated with Agrobacteria transformed with the indicated cYFP-fused and nYFP-CTR1 plasmids and a plasmid expressing the BFP-bZIP reporter protein. Reconstituted YFP fluorescence was observed 3 days after incubation using confocal microscopy. COP1-Interacting Protein 8 (CIP8) was used as a negative control. Scale bars, 100 μm. (B) Co-immunoprecipitation of CTR1 and NPH3. Arabidopsis protoplasts were transfected with GFP only or GFP-fused NPH3 together with Myc tag-fused CTR1. GFP was pulled down with GFP-Trap magnetic agarose, and Myc-CTR1 was detected with an anti-Myc antibody. (C) Co-IP of CTR1 and DRP3A. Arabidopsis protoplasts were transfected with HA tag only or HA tag-fused DRP3A together with Myc tag-fused CTR1. HA tag was pulled down with anti-HA magnetic beads and Myc-CTR1 was detected with an anti-Myc antibody.

increase in the expression of several mitochondrial genes [44, 45]. One study has indicated that the AP2/ERF family of transcription factors, which are downstream targets of the ethylene signaling pathway, may play a role in this process, but the specific mechanism remains to be fully understood [44].

The presence of high-confidence candidate proteins within organelles, such as the mitochondria, raises questions about the localization of CTR1. CTR1 lacks any known organelle targeting sequences, making it unclear how it enters these organelles for interactions with the candidate proteins. Nonetheless, CTR1 can translocate from the ER to the nucleus without any known canonical nuclear localization sequence, where it interacts with EBF1/2, nuclear-localized F-box proteins [5]. One possible scenario for the interaction of CTR1 with proteins localized in organelles, including the nucleus, is that CTR1 may form a complex with cytoplasmic proteins targeted to specific organelles, facilitating its transport and localization through phosphorylation. Alternatively, CTR1 might localize to these organelles through non-canonical import mechanisms. For instance, proteins

can enter the mitochondria through various mechanisms, such as the translocase of the outer membrane (TOM) and the translocase of the inner membrane (TIM), signal peptide-mediated import, being embedded in the phospholipid bilayer of the outer membrane, or chaperone-mediated transport [46, 47]. The identification of TIM44-2 as a high confidence protein candidate supports the possibility that CTR1 enters mitochondria through the TOM-TIM machinery, although further study is required to address this. The localization of mammalian Raf kinases in the mitochondria has been demonstrated by their binding to specific mitochondrial proteins, such as voltage-dependent anion-selective channel 1 (VDAC1) and apoptosis regulator Bcl-2 [48, 49]. They are also recruited to the TOM complex, which enables their localization to the mitochondria and potentially regulates respiration [49]. A-Raf, a member of the Raf kinase family, has also been observed inside the mitochondria and shown to interact with hTIM [50]. Given the structural similarity between CTR1 and Raf kinases, it is possible that CTR1 localizes to the mitochondria in a manner similar to mammalian Raf kinases [10]. It is also possible that CTR1 shares evolutionarily conserved functions with the Raf kinases in terms of its association with mitochondria and its role in regulating respiration. However, further studies are required to fully understand the nature of the proximal interaction between CTR1 and the identified candidate proteins in cellular organelles identified in this study.

While the post-transcriptional regulation of the ethylene signaling pathway has received less attention compared to the regulation of protein stability and gene expression, recent studies have demonstrated positive regulation of the ethylene response occurring at P-bodies. This regulation involves the repression of the translation of *EBF* mRNA, a negative regulator of the pathway, by EIN2 and EIN5 [4, 6]. Notably, three subunits of the CCR4-NOT complex, NOT1, NOT2a, and NOT3, were identified as high-confidence proximal proteins of CTR1. The CCR4-NOT complex is a multi-subunit complex that plays a role in the post-transcriptional regulation of gene expression in eukaryotes [35]. It functions in mRNA degradation through its associated deadenylase and exonuclease enzymes, as well as in other aspects of mRNA metabolism such as transcriptional regulation, mRNA stability, and mRNA localization [33, 35]. The presence of CCR4-NOT complex components as proximal proteins of CTR1 suggests that the post-transcriptional regulation likely contributes to the modulation of ethylene responses. CTR1 may participate in this process by regulating the activity or stability of the CCR4-NOT complex, thereby post-transcriptionally controlling ethylene-responsive genes.

It is not uncommon for proteins to localize in multiple subcellular compartments, enabling them to perform diverse functions in various cellular processes. For instance, Protein Kinase C epsilon is known to be present in the Golgi, plasma membrane, mitochondria, and nucleus [51–54]. The relocation of cytosolic CTR1 to the ER and its subsequent translocation from the ER to the nucleus could potentially result in CTR1 localization to various organelles or cellular structures in the cytoplasm. The findings presented in this study support this possibility. However, we cannot completely rule out the likelihood that some of the proximal proteins to CTR1 resulted from the overexpression of CTR1 in a transient assay. Although we used a native promoter to drive the expression of both GFP-TurboID-CTR1 and GFP-TurboID, the transient expression via agroinfiltration might have led to excessive protein levels within the cells, potentially causing ectopic expression of CTR1. We demonstrated that not all of the selected candidate proteins, such as LON4, exhibited a direct interaction with CTR1. This suggests that LON4 might have been identified as a result of an indirect interaction with CTR1 or due to non-specific interactions caused by the overexpression of CTR1. Therefore, further investigations are necessary to validate the in vivo function of CTR1 in these subcellular localizations.

5 | CONCLUSION

In summary, we employed proximity labeling of CTR1 with TurboID-labeled CTR1, expressed transiently in *N. benthamiana* to identify a group of proteins associated with CTR1 in different subcellular localizations. The identified proteins display diverse subcellular localizations and functions, particularly in mitochondrial respiration and mRNA metabolism. This suggests that CTR1 may have a broader impact on various cellular processes beyond its role in regulating the ethylene signaling pathway. Although these results may not fully represent CTR1 and its associated proteins in other plant species, such as *Arabidopsis*, similar findings are expected, given the high conservation of the ethylene signaling pathway in higher plants [1]. Further investigation is needed to gain a deeper understanding of the role of CTR1 in various cellular processes, including its genetic and biochemical interactions with the identified proximal proteins, as well as the dynamic and spatiotemporal nature of these interactions in intact plants.

AUTHOR CONTRIBUTIONS

G.M.Y. and Y.C. conceived the experimental concept. G.M.Y. supervised the experiments. Y.C. conducted most of the experiments except mass spectrometry. A.R. and S.X. performed the mass spectrometry, analyzed the data, and wrote the related methods. H.L.P. conducted the BiFC and physiology experiments. Y.C. drafted the manuscript, prepared the figures, and edited the manuscript. G.M.Y. edited the manuscript.

ACKNOWLEDGMENTS

This work was supported by grants from the National Science Foundation (MCB-1817286 & IOS-2245525) to G.M.Y. and by the National Institutes of Health grants R01GM135706 to S.-L.X. and diversity supplement to support A.V.R and by the Carnegie Endowment Fund to the Carnegie Mass Spectrometry Facility. The authors thank Purdue Imaging Facility for the confocal microscope service.

CONFLICT OF INTEREST STATEMENT

The authors declare no conflicts of interest.

DATA AVAILABILITY STATEMENT

The raw mass spectrometry proteomics data have been deposited in the ProteomeXchange Consortium via the PRIDE partner repository with the dataset identified PXD041666. All the other data supporting

the findings of this study are available within the paper and its supplementary data published online.

ORCID

Gyeong Mee Yoon https://orcid.org/0000-0003-3936-0700

REFERENCES

1. Abeles, F. B., Morgan, P. W., & Saltveit, M. E. J. (1992). *Ethylene in plant biology*. Academic Press.
2. Alonso, J. M., & Ecker, J. R. (2001). The ethylene pathway: A paradigm for plant hormone signaling and interaction. *Science's STKE: Signal Transduction Knowledge Environment*, *2001*, re1.
3. Wen, X., Zhang, C., Ji, Y., Zhao, Q., He, W., An, F., Jiang, L., & Guo, H. (2012). Activation of ethylene signaling is mediated by nuclear translocation of the cleaved EIN2 carboxyl terminus. *Cell Research*, *22*, 1613–1616.
4. Li, W., Ma, M., Feng, Y., Li, H., Wang, Y., Ma, Y., Li, M., An, F., & Guo, H. (2015). EIN2-directed translational regulation of ethylene signaling in Arabidopsis. *Cell*, *163*, 670–683.
5. Park, H. L., Seo, D. H., Lee, H. Y., Bakshi, A., Park, C., Chien, Y.-C., Kieber, J. J., Binder, B. M., & Yoon, G. M. (2023). Ethylene-triggered subcellular trafficking of CTR1 enhances the response to ethylene gas. *Nature Communications*, *14*, 365.
6. Merchante, C., Brumos, J., Yun, J., Hu, Q., Spencer, K. R., Enríquez, P., Binder, B. M., Heber, S., Stepanova, A. N., & Alonso, J. M. (2015). Gene-specific translation regulation mediated by the hormone-signaling molecule EIN2. *Cell*, *163*, 684–697.
7. Qiao, H., Shen, Z., Huang, S.-S. C., Schmitz, R. J., Urich, M. A., Briggs, S. P., & Ecker, J. R. (2012). Processing and subcellular trafficking of ER-tethered EIN2 control response to ethylene gas. *Science (New York, N.Y.)*, *338*, 390–393.
8. Ju, C., Yoon, G. M., Shemansky, J. M., Lin, D. Y., Ying, Z. I., Chang, J., Garrett, W. M., Kessenbrock, M., Groth, G., Tucker, M. L., Cooper, B., Kieber, J. J., & Chang, C. (2012). CTR1 phosphorylates the central regulator EIN2 to control ethylene hormone signaling from the ER membrane to the nucleus in Arabidopsis. Proceedings of the National Academy of Sciences of the United States of America, *109*, 19486–19491.
9. Alonso, J. M., Hirayama, T., Roman, G., Nourizadeh, S., & Ecker, J. R. (1999). EIN2, a bifunctional transducer of ethylene and stress responses in Arabidopsis. *Science (New York, N.Y.)*, *284*, 2148–2152.
10. Kieber, J. J., Rothenberg, M., Roman, G., Feldmann, K. A., & Ecker, J. R. (1993). CTR1, a negative regulator of the ethylene response pathway in Arabidopsis, encodes a member of the raf family of protein kinases. *Cell*, *72*, 427–441.
11. Chao, Q., Rothenberg, M., Solano, R., Roman, G., Terzaghi, W., & Ecker, J. R. (1997). Activation of the ethylene gas response pathway in Arabidopsis by the nuclear protein ETHYLENE-INSENSITIVE3 and related proteins. *Cell*, *89*, 1133–1144.
12. Berggård, T., Linse, S., & James, P. (2007). Methods for the detection and analysis of protein–protein interactions. *Proteomics*, *7*, 2833–2842.
13. Meyer, K., & Selbach, M. (2015). Quantitative affinity purification mass spectrometry: A versatile technology to study protein-protein interactions. *Frontiers in Genetics*, *6*, 237.
14. Morris, J. H., Knudsen, G. M., Verschueren, E., Johnson, J. R., Cimermancic, P., Greninger, A. L., & Pico, A. R. (2014). Affinity purification–mass spectrometry and network analysis to understand protein-protein interactions. *Nature Protocols*, *9*, 2539–2554.
15. Choi, H., Liu, G., Mellacheruvu, D., Tyers, M., Gingras, A.-C., & Nesvizhskii, A. I. (2012). Analyzing protein-protein interactions from affinity purification-mass spectrometry data with SAINT. *CP in Bioinformatics*, *Chapter 8*, 8.15.11–18.15.23.
16. Kerbler, S. M., Natale, R., Fernie, A. R., & Zhang, Y. (2021). From affinity to proximity techniques to investigate protein complexes in plants. *International journal of molecular sciences*, *22*, 7101.
17. Low, T. Y., Syafruddin, S. E., Mohtar, M. A., Vellaichamy, A., A Rahman, N. S., Pung, Y.-F., & Tan, C. S. H. (2021). Recent progress in mass spectrometry-based strategies for elucidating protein–protein interactions. *Cellular and Molecular Life Sciences*, *78*, 5325–5339.
18. Yang, X., Wen, Z., Zhang, D., Li, Z., Li, D., Nagalakshmi, U., Dinesh-Kumar, S. P., & Zhang, Y. (2021). Proximity labeling: An emerging tool for probing in planta molecular interactions. *Plant Communications*, *2*, 100137.
19. Zhang, Y., Li, Y., Yang, X., Wen, Z., Nagalakshmi, U., & Dinesh-Kumar, S. P. (2020). TurboID-based proximity labeling for in planta identification of protein-protein interaction networks. *Journal of Visualized Experiments: JoVE*, (159), e60728, https://doi.org/10.3791/60728
20. Mair, A., Xu, S. L., Branon, T. C., Ting, A. Y., & Bergmann, D. C. (2019). Proximity labeling of protein complexes and cell-type-specific organellar proteomes in Arabidopsis enabled by TurboID. *Elife*, *8*, e47864.
21. Liu, X., Salokas, K., Weldatsadik, R. G., Gawriyski, L., & Varjosalo, M. (2020). Combined proximity labeling and affinity purification-mass spectrometry workflow for mapping and visualizing protein interaction networks. *Nature Protocols*, *15*, 3182–3211.
22. Branon, T. C., Bosch, J. A., Sanchez, A. D., Udeshi, N. D., Svinkina, T., Carr, S. A., Feldman, J. L., Perrimon, N., & Ting, A. Y. (2018). Efficient proximity labeling in living cells and organisms with TurboID. *Nature Biotechnology*, *36*, 880–887.
23. Oakley, J. V., Buksh, B. F., Fernández, D. F., Oblinsky, D. G., Seath, C. P., Geri, J. B., Scholes, G. D., & MacMillan, D. W. C. (2022). Radius measurement via super-resolution microscopy enables the development of a variable radii proximity labeling platform. Proceedings of the National Academy of Sciences of the United States of America, *119*, e2203027119.
24. Heberle, H., Meirelles, G. V., Da Silva, F. R., Telles, G. P., & Minghim, R. (2015). InteractiVenn: A web-based tool for the analysis of sets through Venn diagrams. *BMC Bioinformatics [Electronic Resource]*, *16*, 169.
25. UniProt Consortium. (2015). UniProt: A hub for protein information. *Nucleic Acids Research*, *43*, D204–D212.
26. Szklarczyk, D., Gable, A. L., Lyon, D., Junge, A., Wyder, S., Huerta-Cepas, J., Simonovic, M., Doncheva, N. T., Morris, J. H., Bork, P., Jensen, L. J., & Mering, C. V. (2019). STRING v11: Protein–protein association networks with increased coverage, supporting functional discovery in genome-wide experimental datasets. *Nucleic Acids Research*, *47*, D607–d613.
27. Hawkins, C., Ginzburg, D., Zhao, K., Dwyer, W., Xue, B., Xu, A., Rice, S., Cole, B., Paley, S., Karp, P., & Rhee, S. Y. (2021). Plant Metabolic Network 15: A resource of genome-wide metabolism databases for 126 plants and algae. *Journal of Integrative Plant Biology*, *63*, 1888–1905.
28. Yoo, S.-D., Cho, Y.-H., & Sheen, J. (2007). Arabidopsis mesophyll protoplasts: A versatile cell system for transient gene expression analysis. *Nature Protocols*, *2*, 1565–1572.
29. Botha, F. C., Potgieter, G. P., & Botha, A. M. (1992). Respiratory metabolism and gene expression during seed germination. *Plant Growth Regulation*, *11*, 211–224.
30. Martínez-Reyes, I., & Chandel, N. S. (2020). Mitochondrial TCA cycle metabolites control physiology and disease. *Nature Communications*, *11*, 102.
31. Rigas, S., Daras, G., Tsitsekian, D., Alatzas, A., & Hatzopoulos, P. (2014). Evolution and significance of the Lon gene family in Arabidopsis organelle biogenesis and energy metabolism. *Frontiers in Plant Science*, *5*, 145.
32. Van Wijk, K. J. (2015). Protein maturation and proteolysis in plant plastids, mitochondria, and peroxisomes. *Annual Review of Plant Biology*, *66*, 75–111.

33. Traven, A., Beilharz, T. H., Lo, T. L., Lueder, F., Preiss, T., & Heierhorst, J. R. (2009). The Ccr4-Pop2-NOT mRNA deadenylase contributes to septin organization in Saccharomyces cerevisiae. *Genetics*, *182*, 955–966.
34. Chalabi Hagkarim, N., & Grand, R. J. (2020). The Regulatory Properties of the Ccr4-Not Complex. *Cells*, *9*(11), 2379.
35. Collart, M. A. (2016). The Ccr4-Not complex is a key regulator of eukaryotic gene expression. *Wiley Interdiscip Rev RNA*, *7*, 438–454.
36. Miller, J. E., & Reese, J. C. (2012). Ccr4-Not complex: The control freak of eukaryotic cells. *Critical Reviews in Biochemistry and Molecular Biology*, *47*, 315–333.
37. Mair, A., & Bergmann, D. C. (2022). Advances in enzyme-mediated proximity labeling and its potential for plant research. *Plant Physiology*, *188*, 756–768.
38. Haga, K., Tsuchida-Mayama, T., Yamada, M., & Sakai, T. (2015). Arabidopsis ROOT PHOTOTROPISM2 Contributes to the Adaptation to High-Intensity Light in Phototropic Responses. *Plant Cell*, *27*, 1098–1112.
39. Sullivan, S., Kharshiing, E., Laird, J., Sakai, T., & Christie, J. M. (2019). Deetiolation Enhances Phototropism by Modulating NON-PHOTOTROPIC HYPOCOTYL3 Phosphorylation Status. *Plant Physiology*, *180*, 1119–1131.
40. Sullivan, S., Waksman, T., Paliogianni, D., Henderson, L., Lütkemeyer, M., Suetsugu, N., & Christie, J. M. (2021). Regulation of plant phototropic growth by NPH3/RPT2-like substrate phosphorylation and 14-3-3 binding. *Nature Communications*, *12*, 6129.
41. Nelson, B. K., Cai, X., & Nebenführ, A. (2007). A multicolored set of in vivo organelle markers for co-localization studies in Arabidopsis and other plants. *Plant Journal*, *51*, 1126–1136.
42. Mano, S., Nakamori, C., Kondo, M., Hayashi, M., & Nishimura, M. (2004). An Arabidopsis dynamin-related protein, DRP3A, controls both peroxisomal and mitochondrial division. *Plant Journal*, *38*, 487–498.
43. Gao, Z., Chen, Y.-F., Randlett, M. D., Zhao, X.-C., Findell, J. L., Kieber, J. J., & Schaller, G. E. (2003). Localization of the Raf-like kinase CTR1 to the endoplasmic reticulum of Arabidopsis through participation in ethylene receptor signaling complexes. *Journal of Biological Chemistry*, *278*, 34725–34732.
44. Wang, X., & Auwerx, J. (2017). Systems phytohormone responses to mitochondrial proteotoxic stress. *Molecular Cell*, *68*, 540–551.e5.e545.
45. Yu, L., Liu, Y., & Xu, F. (2019). Comparative transcriptome analysis reveals significant differences in the regulation of gene expression between hydrogen cyanide- and ethylene-treated Arabidopsis thaliana. *BMC Plant Biology*, *19*, 92.
46. Schmidt, O., Pfanner, N., & Meisinger, C. (2010). Mitochondrial protein import: From proteomics to functional mechanisms. *Nature Reviews Molecular Cell Biology*, *11*, 655–667.
47. Zhao, F., & Zou, M. H. (2021). Role of the mitochondrial protein import machinery and protein processing in heart disease. *Frontiers in Cardiovascular Medicine*, *8*, 749756.
48. Shoshan-Barmatz, V., Krelin, Y., Shteinfer-Kuzmine, A., & Arif, T. (2017). Voltage-dependent anion channel 1 as an emerging drug target for novel anti-cancer therapeutics. *Frontiers in Oncology*, *7*, 154.
49. Galmiche, A., & Fueller, J. (2007). RAF kinases and mitochondria. *Biochimica Et Biophysica Acta*, *1773*, 1256–1262.
50. Yuryev, A., Ono, M., Goff, S. A., Macaluso, F., & Wennogle, L. P. (2000). Isoform-specific localization of A-RAF in mitochondria. *Molecular and Cellular Biology*, *20*, 4870–4878.
51. Lehel, C., Olah, Z., Jakab, G., & Anderson, W. B. (1995). Protein kinase C epsilon is localized to the Golgi via its zinc-finger domain and modulates Golgi function. Proceedings of the National Academy of Sciences of the United States of America, *92*, 1406–1410.
52. Beckmann, R., Lindschau, C., Haller, H., Hucho, F., & Buchner, K. (1994). Differential nuclear localization of protein kinase C isoforms in neuroblastoma x glioma hybrid cells. *European Journal of Biochemistry*, *222*, 335–343.
53. Di Marcantonio, D., Martinez, E., Sidoli, S., Vadaketh, J., Nieborowska-Skorska, M., Gupta, A., Meadows, J. M., Ferraro, F., Masselli, E., Challen, G. A., Milsom, M. D., Scholl, C., Fröhling, S., Balachandran, S., Skorski, T., Garcia, B. A., Mirandola, P., Gobbi, G., Garzon, R., & Sykes, S. M. (2018). Protein Kinase C Epsilon is a key regulator of mitochondrial redox homeostasis in acute myeloid leukemia. *Clinical Cancer Research*, *24*, 608–618.
54. D'Amico, A. E., & Lennartz, M. R. (2018). Protein kinase C-epsilon in membrane delivery during phagocytosis. *Journal of Immunological Sciences*, *2*, 26–32.

SUPPORTING INFORMATION

Additional supporting information may be found online https://doi.org/10.1002/pmic.202300212 in the Supporting Information section at the end of the article.

How to cite this article: Chien, Y.-C., Reyes, A., Park, H. L., Xu, S.-L., & Yoon, G. M. (2024). Uncovering the proximal proteome of CTR1 through TurboID-mediated proximity labeling. *Proteomics*, *24*, e2300212. https://doi.org/10.1002/pmic.202300212